

# The Fluidization Properties of Bagasse Pulp Suspensions in a Rotary Device

Zhi Li,<sup>a,b</sup> Jun Li,<sup>a,b</sup> Jun Xu,<sup>a,b,\*</sup> Li-huan Mo,<sup>a,b</sup> Yu-cheng Feng,<sup>a,b</sup> and Ke-fu Chen<sup>a,b</sup>

Suspensions of bleached bagasse pulp at 0% to 15% mass concentrations were sheared in a concentric cylinder rotary device to study the pulp suspension's fluidization properties. The use of a baffled chamber, with blade rotors, imposed shear stress within the suspensions and prevented slip at the chamber walls. Linear-type, hollow-type, and screw-type rotors were used to explore the influence of rotor structure on fluidization properties. The torque was measured as a function of rotational speed. The torque vs. rotational speed curves and flow phenomenon were found to depend on the mass consistency of the pulp suspensions and the gap between the rotor and chamber. The structure of the rotor had little influence on the fluidization of the pulp suspensions, and the critical rotational speed that makes the pulp suspensions turbulent was similar for all rotor types. The gap between the rotor and chamber should be small to let pulp suspensions fluidize at low rotational speed.

*Keywords:* Bagasse pulp; Fluidization; Rotational shear; Fluidizer

*Contact information:* a: State Key Laboratory of Pulp and Paper Engineer, South China University of Technology, Guangzhou 510640, China; b: United Lab of Plant Resources Chemistry and Chemical Engineering, South China University of Technology, Guangzhou 510640, China;

\* Corresponding author: xujun@scut.edu.cn

## INTRODUCTION

The flow of fiber suspensions is a key factor in the pulp and paper industry. The production of papermaking pulp involves the handling of large quantities of fiber suspensions. Today's call for energy efficiency and environmentally sound processes has led to the development of Medium Consistency (MC) technology (Sixta *et al.* 1991; Behrooz *et al.* 2012; Li *et al.* 2015). Most unit operations in the pulp industry are now routinely performed at concentrations higher than 10%, at which pulp suspensions are a three-phase heterogeneous mixture of water, fiber, and air (Kerekes *et al.* 1985; Lindsay *et al.* 1995). Fiber orientation and migration away from solid boundaries creates a depletion layer near walls, which makes the rheology of pulp suspensions complex (Wikstrom *et al.* 1998; Sampson 2001; Cui and Grace 2007; Hubbe 2007). The rheological measurements on medium and high consistency pulp suspensions is limited.

Medium consistency pulp suspensions behave like a solid in the steady flow state, where individual fibers are entangled with each other, forming a network plug that has a structure to resist deformation (Hietaniemi and Gullichsen 1996). However, fluid-like motion can be created by exceeding the pulp suspension's yield stress and imposing sufficient shear forces to maintain fiber motion by continually rupturing the suspensions. Gullichsen and Harkonen (1981) concluded that there are no fundamental differences between low (0% to 6%) and medium (8% to 15%) consistency fiber suspensions with regard to their response to shear forces, and the hydrodynamic properties of turbulent

fiber suspensions resemble those of water. The imposition of relative motion in fiber suspensions and resulting fluid-like properties have been called “fluidization”. In the pulp and paper literature, the term “fluidization” has become synonymous with the creation of a fluid-like state in a pulp suspension. In particular, the term is used to imply creation of a water-like motion in the medium consistency pulp suspensions that are otherwise regarded as solid-like. Based on Gullichsen’s findings, later works have studied fluidization in more detail. Bennington *et al.* (1991) have observed fibre-level fluidization at the rotor vane tips and largely floc-level fluidization in zones away from the rotor. Hietaniemi and Gullichsen (1996), and Chen and Chen (1997) measured the onset of fluidization using a vaned narrow-gap viscometer. Wikstrom and Rasmuson (2002) modelled the flow inside a pulp pressure screen with a computational fluid dynamics (CFD) model incorporating both laminar and turbulent conditions. New process equipment was quickly developed to exploit these findings. Machinery to pump and mix MC pulp suspensions, employing centrifugal motion to provide fluidization, are now in widespread use.

To measure the fluidization properties of pulp suspensions, most researchers have used vaned geometry devices (Bennington *et al.* 1995; Derakhshandeh *et al.* 2010). However, according to their experimental devices, the structure of rotors was settled. According to previous investigations by the authors, the turbulence generator of MC pump had many different structures, and MC pump was developed based on fluidization theory, so it was of interest to find out whether the rotor geometry would have an influence on the fluidization properties of MC pulp suspensions. Besides, most of the previous studies were focused on wood pulp, and little research has been published on medium consistency, non-wood bagasse pulp suspensions under conditions of high shear. The following work was intended to provide a better understanding of the fluidization behavior of bagasse pulp suspensions and the influence of rotor structures on pulp suspensions’ fluidization properties.

## EXPERIMENTAL

### Materials

Bleached bagasse pulp (soda pulping technology) was studied in these experiments. Samples of bleached bagasse pulp were obtained from a pulp plant located in Guangxi Province, China. The pulp was dewatered to a consistency of approximately 30% and stored in sealed-plastic bags. The pulp had a drainage of 18.2 °SR, and fiber length (weighted average fiber length by weight) was 1.01 mm.

### Equipment

Fluidization experiments were conducted in an experimental device called the “fluidizer”, which was made in the laboratory. A schematic diagram and a photograph of the pulp fluidizer are presented in Fig. 1. The fluidizer is powered by a 5.0-kW variable speed alternating current (AC) motor which permitted the rotors attached to the shaft to reach speeds of up to 3000 rpm. The pulp suspensions were contained in a chamber formed between the rotor and the vessel wall. The rotor had blades that protruded into the pulp suspensions to prevent suspension slippage at the rotor/suspensions interface, while the chamber was baffled to prevent fiber slippage at the outer wall. A shear field was generated between the rotational rotor and the housing wall. A torque meter was installed

between the rotor and the motor, and it was used to measure the torque of the pulp suspension. The torque and rotational speed, in real time, are sent to the data acquisition system. A clear sight glass was installed in the top of the fluidizer, permitting observation of the pulp suspension.

Three rotors, with different structures, were used to explore the influence of rotor structure on the fluidization properties of pulp suspensions. The specific three rotor models are shown in Fig. 2. Figure 2 (a) shows a linear-type rotor with two symmetrical blades, (b) is a hollow-type rotor with three blades distributed in 360 degree uniformity, and (c) is a screw-type rotor with two symmetrical helical blades. All the rotors have the same blade diameter, width, and height. The height of the rotor was equal to the height of the vessel chamber. The vessel chamber diameter was 105 mm and its height was 117 mm, the diameter of the rotor shaft was 35 mm, the blade width was 20 mm, and the baffle width of chamber was 10 mm, and the gap between chamber baffle and rotor blade was 5 mm.

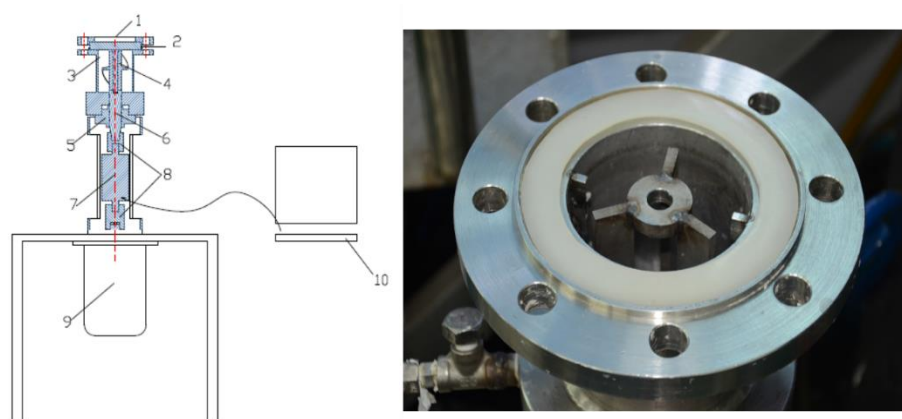


**Fig. 1.** Schematic diagram and a photograph of the pulp fluidizer: 1. flange cover; 2. sight glass; 3. vessel chamber; 4. rotor; 5. mechanical seal and bearing; 6. shaft; 7. torque meter; 8. coupler; 9. AV motor; 10. data acquisition system

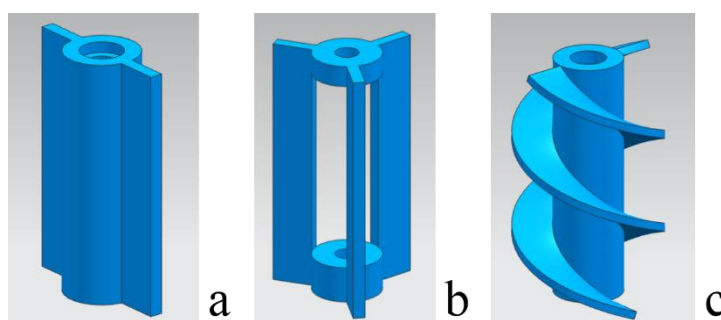


**Fig. 2.** Pulp fluidizer rotors used in the experiment: (a) linear-type rotor, (b) hollow-type rotor, (c) screw-type rotor

## Methods

Pulp suspensions were added to the fluidizer from the top of the chamber. It was important that the chamber was completely filled with the pulp suspension. The covered sight glass was then screwed on with bolts in order to prevent the pulp suspensions from spilling out of the chamber. The rotor rotational speed was set at several specific values

varying from 0 rpm to 3000 rpm and rotated for about 10 s at each specific rotational speed. Shaft torque data and rotational speed data were acquired every 500 ms by a data acquisition system. The net torque was calculated by subtracting the frictional torque from the total torque. In addition, the pulp suspensions samples should only be used one time at a specific rotational speed and consistency. Fibre length was measured by using a Kajaani FS300 type fibre analyzer (Metso, Kajaani/Finland). Consistency (concentration) of pulp suspensions was evaluated using TAPPI standard T240 om-2. Beating degree was evaluated using GB/T 3332-1982.

## RESULTS AND DISCUSSION

### Preliminary Tests

During the initial tests, it was found that the experimental data were difficult to quantify. Some typical torque vs. rotational time curves for the preliminary test are given in Fig. 3, for a 12%  $C_m$  (mass consistency, mass of fiber divided by the total mass of suspension) bleached bagasse pulp with the linear-type rotor. Figure 3 shows that the torque decreased gradually with the increasing of the rotational time at a constant rotational speed. In addition, the torque showed apparent swings at rotational speeds of 1500 and 2000 rpm. Therefore, defining the measured torque values at specific rotational speeds is a problem.

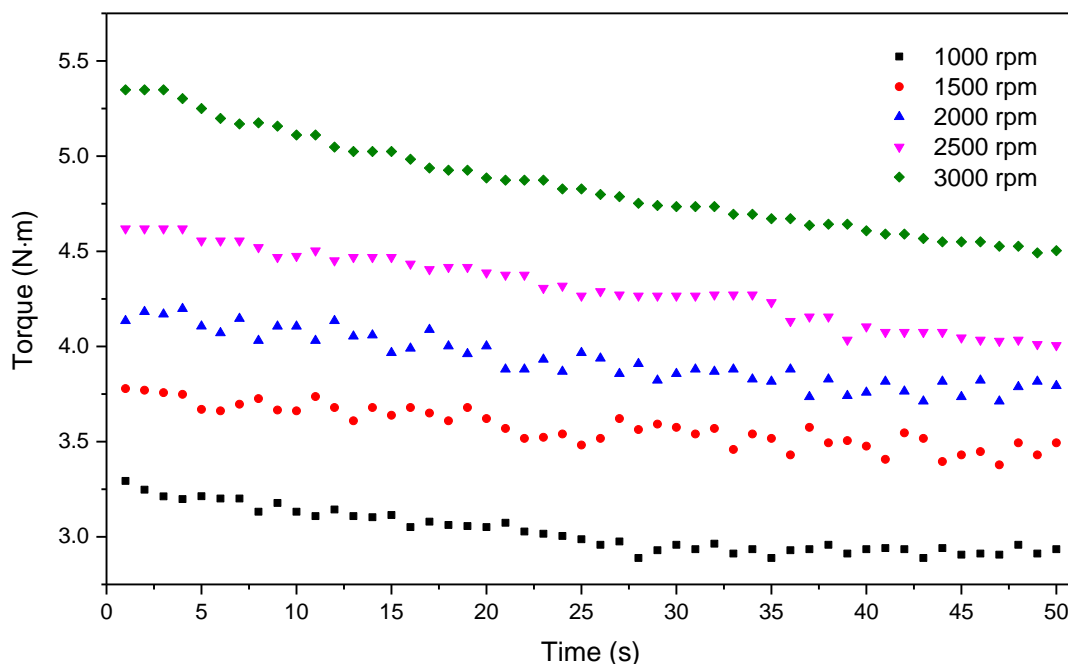


**Fig. 3.** Torque vs. rotational time curves for bleached bagasse pulp suspensions of  $C_m=12\%$ . Tests for 1000 rpm, 1500 rpm, 2000 rpm, 2500 rpm, and 3000 rpm are shown. A linear-type rotor was used in the tests.

The above apparent thixotropic (shear thinning) behavior was not observed for tests made with a Newtonian fluid (water), and is attributed to a number of factors.

Changes in fiber properties resulted from stress during the test period. The amount of fiber degradation increased with mechanical treatment. The fiber length and

beating degree vs. rotational speed curves are shown in Fig. 4, wherein fiber length decreased with the rotational speed, while beating degree increased with the increase of the rotational speed. The gap between the rotor blade and chamber baffle was very small (5 mm). As rotational time went on, more shear stress was imposed on the fiber, the friction probability between fibers was also increased, more fibers were cut off, the fiber lengths shortened, and the interleaving force between fibers decreased greatly, so the torque would decrease.

An increase in suspension temperature was caused by energy dissipation. As the energy expended, which created flow, it is ultimately dissipated as heat, and the temperature of the suspensions increased substantially. For example, in the fifty second duration of a preliminary test, the temperature of a 5%  $C_m$  bleached bagasse pulp suspensions increased by approximately 6 °C, while approximately a 40 °C increase was observed in a 15% suspension. This temperature increase reduced suspending medium viscosity, which in turn also reduced suspension viscosity. In addition, pulp fibers became more flexible with increasing the temperature which may reduce suspension viscosity as well.

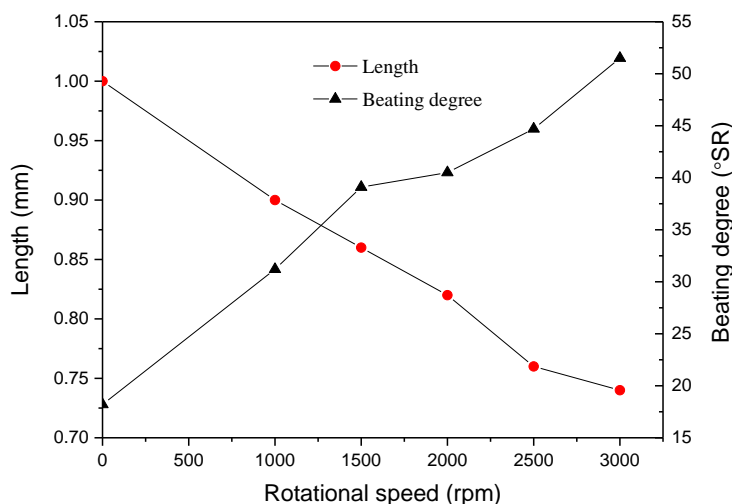


**Fig. 4.** Fiber length and beating degree vs. rotational speeds for bagasse pulp suspensions of  $C_m=12\%$  after rotated 50 s in the fluidizer.

To avoid changes in suspensions behavior arising because of heating and mechanical treatment, it was decided that the test period should be as short as possible. This required a fairly rapid acceleration rate and a short rotational time. As shown in Fig. 3, fiber length had little change in the initial few seconds, therefore, the average of the first five measured torque data points at the set rotational speed were used in the analysis. The pulp suspensions must be changed to perform every shear test at a new point.

### The Fluidization Properties of Bagasse Pulp Suspensions

A bleached bagasse pulp was used for a series of tests in the pulp fluidizer, where pulp suspension's consistencies were varied in steps from 0% to 15%  $C_m$ . The torque vs. rotational speed curves are shown in Fig. 5 for these tests. The curves where rotational speeds below 250 rpm were not drawn because the force supplied by the motor at low rotational speed was not big enough to overcome the inertial forces of the fluidizer and resistance of the pulp network, especially in high consistency range. There were substantial relative errors between measured and set rotational speed. In addition,

according to the previous studies, pulp suspensions shows more yield characteristic in this region, limited by the experiment equipment and data collecting period, so curves in this region were not displayed.

The torque vs. rotational speed curves for the pulp suspensions mainly displayed two flow regimes, divided by a predicted fluidization point. The prediction point of fluidization, as observed at the top face of the fluidizer and deduced from the torque curves, is indicated by the solid black point on each pulp suspensions curve.

As shown in Fig. 5 region 1, as rotational speed was increased, the torque for the pulp curves also increased. The magnitude of the increase was especially significant for higher pulp consistencies. The force supplied by the rotor needed to overcome not only the friction forces between pulp suspension and rotor surface, but also the interaction forces between the flowing fiber network and static fiber network. So, the higher the rotational speed, the higher torque, and the higher consistency were observed. After an initial torque increasing stage, the increasing gradient of the torque became gradual as a result of the decreasing size of the fiber network, so the gradient of shear stress needed for disruption of the fiber network also decreased correspondingly (Chen and Chen 1997). As the rotational speed continued to increase and reach a critical rotational speed value (predicted fluidization point), the pulp curves began to increase sharply and parallel to the water curve. This was mainly due to the fact that when the flowing zone increased with rotational speed and filled the entire chamber, the pulp suspensions in the vessel were sheared strongly, and the flows moved along the axial direction as well as the radial direction; therefore a strong turbulent flow formed. This phenomenon was called fluidization, and the critical rotational speed point was called onset of fluidization. The fluidization properties of bagasse pulp suspensions obtained by this fluidizer was similar with previous studies (Gullichsen and Harkonen 1981).

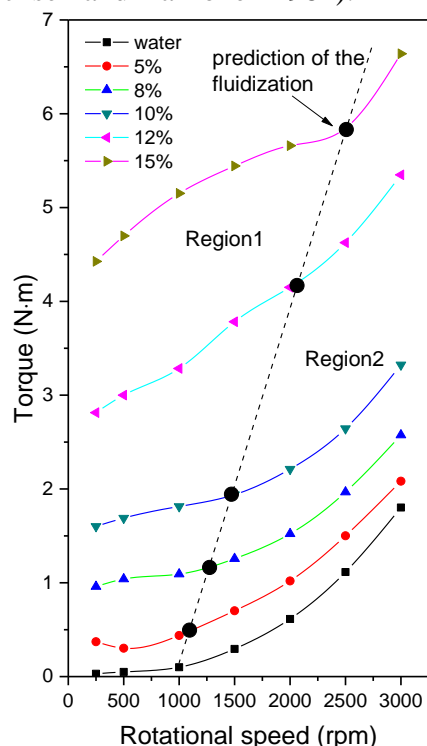


**Fig. 5.** Torque vs. rotational speed curves for bleached bagasse with linear-type rotor. Tests for 0% (water), 5%, 8%, 10%, 12%, and 15%  $C_m$  are shown. The prediction of fluidization is indicated by the solid black point on each pulp suspensions curve.

### The Influence of Rotor Structure on the Fluidization of Pulp Suspensions

Three types of fluidizer rotors were used for the tests to explore whether the rotor structures had influence on the fluidization properties of pulp suspensions. The torque vs. rotational speed curves are shown in Fig. 6 for these tests.

As shown in Figs. 6(a) and (b), in general, the shape of pulp curves obtained by a hollow-type rotor and a screw-type rotor were similar with each other, and they were also similar with the curves obtained by the linear-type rotor. Two flow regimes are shown in the curves. First, increasing torque with the increasing rotational speed caused the gradient to increase gradually until the predicted onset of fluidization. Second, once the rotational speed reached the critical rotational speed point, the torque was dramatically increased and the curves began to parallel to the water curve. By observation from the sight glass in the fluidizer, the critical rotational speed, which made pulp suspensions in the fluidizer fully turbulent, were close although the rotor types were different, which indicated that the fluidization characteristic of pulp suspensions had little relation to the fluidizer rotors type because of the equal key diameters. As long as the rotational speed achieved a critical point, fluidization could be realized.

The torque of the screw-type rotor was higher than linear-type rotor and hollow-type rotor, mostly because that the screw-type rotor not only supplied radial forces but also axial forces, and axial flows were generated with radial flows. Therefore, it was easy to make the suspension fully turbulent with the screw-type rotor, and the required power for the screw-rotor would be higher than linear-type rotor and hollow-type rotor accordingly.

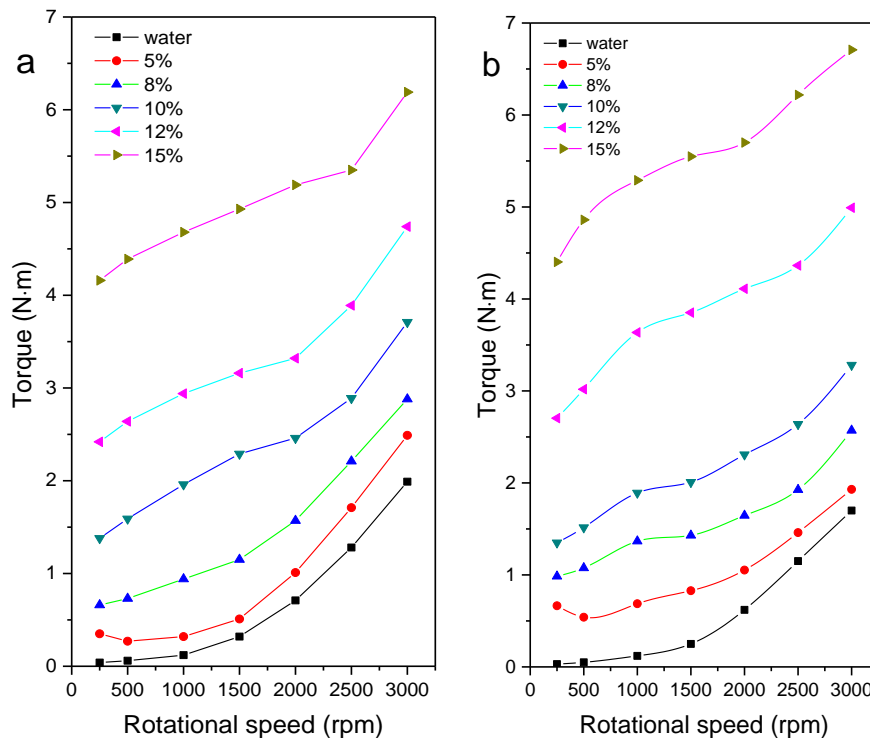


**Fig. 6.** Torque vs. rotational speed curves for bleached bagasse with different type rotors. Tests for 0% (water), 5%, 8%, 10%, 12%, and 15%  $C_m$  are shown. (a) Hollow-type rotor, (b) Screw-type rotor

## Wide-Gap Experiments

The gap between the chamber baffle and rotor blade is another characteristic of rotors which may have an influence on the fluidization characteristic of pulp suspensions. In the following wide-gap experiments, the blade width was 10 mm and the gap between the chamber baffle and rotor blade was 15 mm, which represents an increase of 10 mm compared with narrow-gap experiments. As discussed before, the structure had little influence on the fluidization of pulp suspensions, so, from the aspect of rotor manufacturing, the line-type rotor was the easiest to make, as a result the line-type rotor was used in the following experiment.

Torque vs. rotational speed curves for a series of tests in the wide-gap configuration using bagasse pulp and linear-type rotor are given in Fig. 7. The curves display some of the features observed in the narrow-gap experiments: an increasing torque with increasing rotational speed and pulp consistency. However, the torques tested in the wide-gap experiments were obviously smaller than that in the narrow-gap experiments. In the lower consistency region (5% to 8%), pulp curves were familiar with pulp curves obtained in narrow-gap experiments. The curves for pulp suspensions began to parallel to water curve after the rotational speed exceeded a predicted onset of fluidization, but the predicted onset of fluidization occurred later than that in the narrow-gap experiments. When the consistency was in medium consistency range (10% to 15%), the predicted onset of fluidization did not occur; pulp curves showed a linear growth trend even the rotational speed was 3000 rpm. By observation from the sight glass in the fluidizer, when the rotational speed was up to 3000 rpm, the fully turbulent behavior was not observed in the fluidizer chamber. Part of pulp suspensions that were near the chamber wall were still in the static state, especially for higher consistency pulp suspensions. This is attributed to a number of factors.

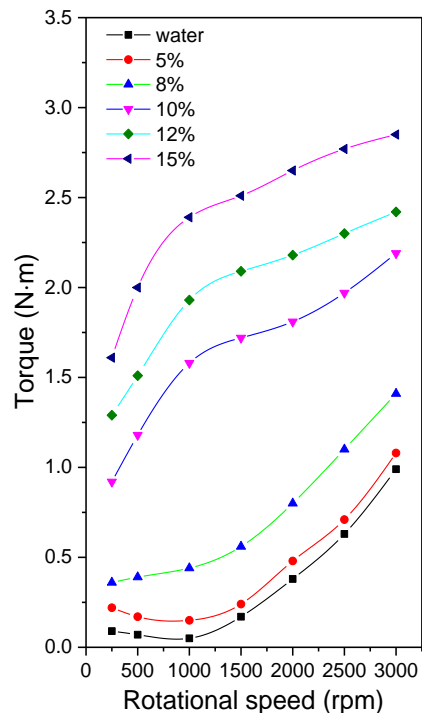


**Fig. 7.** Torque vs. rotational speed curves for bleached bagasse with linear-type rotor in the wide-gap configuration. Tests for 0% (water), 5%, 8%, 10%, 12%, and 15%  $C_m$  are shown.

Changes in blade width caused the shear stress supplied by the rotor to be much smaller than that in the narrow-gap experiments, and therefore the fiber network was not easily fully disrupted. As the consistency increased, the fibers formed many flocs, and the gas content increased; thus the motion was hard to transfer from one floc to another floc.

To better understand the flow regimes of pulp suspensions in the wide-gap and narrow-gap fluidizer, static pictures of pulp suspensions in the top view of fluidizer were taken after the pulp suspensions were rotated at the set rotational speed. An aqueous green dye, initially injected adjacent to the rotor, indicates the radial extent of motion in the suspension. As the zone of motion grew, the radial extent of dye penetration is distinctly visible in the photographs. The black solid line represents the fluidizer chamber wall, and the red broken line represents the mainly fluid-like motion zone. The observed regimes of pulp motion in wide-gap and narrow-gap tests are shown in Figs. 8 and 9.

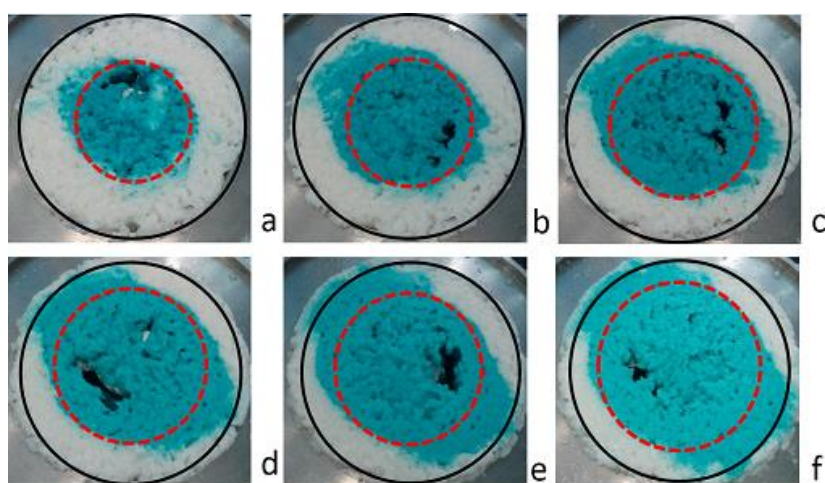


**Fig. 8.** Six pictures taken from a static picture made after the pulp rotated in set rotational speed for a bleached bagasse pulp of  $C_m=15\%$  in a wide-gap fluidizer with a linear-type rotor. Aqueous green dye was initially injected adjacent to the rotor. (a) 500 rpm, (b) 1000 rpm, (c) 1500 rpm, (d) 2000 rpm, (e) 2500 rpm, (f) 3000 rpm

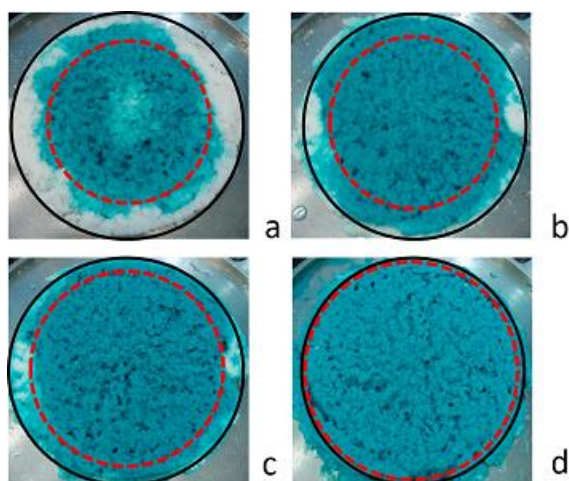


**Fig. 9.** Four pictures taken from a static picture made after the pulp rotated in set rotational speed for a bleached bagasse pulp of  $C_m=15\%$  in a narrow-gap fluidizer with a linear-type rotor. Aqueous green dye was initially injected adjacent to the rotor. (a) 500 rpm, (b) 1000 rpm, (c) 1500 rpm, (d) 2000 rpm

Below the yield stress, the pulp was compressed, and gas pockets appeared behind the rotor blades. After yielding, flocs in the immediate rotor vicinity moved in a rolling, tumbling manner. As rotor speed increased, the motion zone increased in volume as it expanded radially outwards from the rotor. When the flow reached the outer chamber wall, an abrupt flow transition would occur. It can be seen that it was hard to increase the motion zone by increasing rotational speed in the wide-gap experiment. When the rotational speed was up to 3000 rpm, the main rotational region was around the rotor, not reaching the wall; however, in the narrow-gap experiment, the motion zone expanded to the wall and formed strong turbulence when the rotational speed was 2000 rpm. It was concluded that the gap between rotor and chamber wall should be narrow to obtain a turbulent state at relatively low rotational speed.

## CONCLUSIONS

1. Bagasse pulp suspensions containing up to 15%  $C_m$  can be fluidized in a rotary shear tester and display a fluid-like behavior, as reported by earlier workers for other types of pulp.
2. The structure of rotors installed on the fluidizer has little influence on fluidization properties of pulp suspensions, as long as the rotational speed reaches the critical point, fluidization can be realized.
3. The gap between shear chamber wall and rotor should be narrow in order to obtain turbulent state by using low relatively rotational speed.

## ACKNOWLEDGMENTS

The authors are grateful for the support of the China Major Science and Technology Program for Water Pollution Control and Treatment, Grant No. 2014ZX07213001; the Guangzhou Special Support Program, Grant No. 2014TQ01N603; and the Science and Technology Plan Projects of Guangzhou city, Grant No. 201504010013.

## REFERENCES CITED

- Behrooz, R., Ghasemi, S., Atoii, G. A., and Fatehi, P. (2012). "Mg(OH)<sub>2</sub>-based hydrogen peroxide bleaching of CMP pulps at high consistency," *BioResources* 7(1), 161-172. DOI: 10.15376/biores.7.1.161-172
- Bennington, C. P. J., Kerekes, R. J., and Grace, J. R. (1991). "Motion of pulp fiber suspensions in rotary devices," *Canadian Journal of Chemical Engineering* 69(1), 251-258. DOI: 10.1002/cjce.5450690130
- Bennington, C. P. J., Azevedo, G., John, D. A., Birt, S. M., and Wolgast, B. H. (1995). "The yield stress of medium and high consistency mechanical pulp fiber suspensions at high gas contents," *Journal of Pulp and Paper Science* 21(4), 111-118.
- Chen, K. F., and Chen, S. M. (1997). "Fluidization properties of high consistency fiber suspensions," *Experimental Thermal and Fluid Science* 14(2), 149-159.

- Cui, H., and Grace, J. R. (2007). "Flow of pulp fiber suspension and slurries: A review," *International Journal of Multiphase Flow* 33(9), 921-934. DOI: 10.1016/j.ijmultiphaseflow.2007.03.004
- Derakhshandeh, B., Hatzikiriakos, S. G., and Bennington, C. P. J. (2010). "The apparent yield stress of pulp fiber suspensions," *Journal of Rheology* 54(5), 1137-1154. DOI: 10.1122/1.3473923
- Gullichsen, J., and Harkonen, E. (1981). "Medium consistency technology," *TAPPI Journal* 64(6), 69-72.
- Hietaniemi, J., and Gullichsen, J. (1996). "Flow properties of medium-consistency fiber suspensions," *Journal of Pulp and Paper Science* 22(12), 469-474.
- Hubbe, M. A. (2007). "Flocculation and redispersion of cellulosic fiber suspensions: A review of effects of hydrodynamic shear and polyelectrolytes," *BioResources* 2(2), 296-331. DOI: 10.15376/biores.2.2.296-331
- Kerekes, R. J., Soszynski, R. M., and Doo, P. A. T. (1985). "The flocculation of pulp fibers," *Proceedings of the 8<sup>th</sup> Fundamental Research Symposium*, Oxford, UK, pp. 265-310.
- Li, Z., Li, J., Xu, J., and Mo, L. H. (2015). "Clean bleaching engineering practice for bagasse pulp: totally chlorine-free and elemental chlorine-free bleaching realized with the same production line," *BioResources* 10(2), 2667-2680. DOI: 10.15376/biores.10.2.2667-2680
- Lindsay, J. D., Ghiaasiaan, S. M., and Abdel-Khalik, S. I. (1995). "Macroscopic flow structures in a bubbling paper pulp-water slurry," *Industrial and Engineering Chemistry Research* 34(10), 3342-3354. DOI: 10.1021/ie00037a021
- Sampson, W. W. (2001). "The structural characterization of fiber networks in papermaking processes – A review," *Proceedings of the Transactions of 12<sup>th</sup> Fundamental Resource Symposium*, Oxford, UK, pp. 1205-1288.
- Sixta, H., Goetzinger, G., Schrittwieser, A., and Hendel, P. (1991). "Medium consistency ozone bleaching: Laboratory and mill experience," *Papier* 45(10), 610-625.
- Wikstrom, T., Defibrator, S., and Rasmuson, A. (1998). "Yield stress of pulp suspensions: The influence of fiber properties and processing conditions," *Nordic Pulp and Paper Research Journal* 13(3), 243-250. DOI: 10.3183/NPPRJ-1998-13-03-p243-246
- Wikstrom, T., and Rasmuson, A. (2002). "Transition modelling of pulp suspensions applied to a pressure screen," *Journal of Pulp and Paper Science* 28(11), 374-378.

Article submitted: November 17, 2015; Peer review completed: December 30, 2015;  
Revised version received: January 7, 2016; Accepted: January 11, 2016; Published:  
January 28, 2016.

DOI: 10.15376/biores.11.1.2629-2639